UNIVERSIDAD DE CONCEPCIÓN
FACULTAD DE INGENIERÍA
DEPARTAMENTO DE INGENIERÍA MECÁNICA

MODELLING OF MOTORCYCLE DYNAMICS IN STRAIGHT RUNNING AND STEADY CORNERING FOR LATERAL STABILITY ANALYSIS

Por

Benjamín Eimol González Toledo

Memoria de Título presentada a la Facultad de Ingeniería de la Universidad de Concepción para optar al título profesional de Ingeniero Civil Mecánico

Profesores Guía:
PhD Felipe Vásquez
PhD Bernardo Hernández

Diciembre 2023
Concepción, Chile

A todos los que estuvieron en el proceso.

ACKNOWLEDGEMENTS

Me gustaría agradecer a mi familia por todo el apoyo y motivación durante estos años universitarios. Sin duda alguna, es gracias a ustedes que hoy termino este viaje.

A mis queridos amigos del grupo "vamos joder" por tanta ayuda y paciencia en cada trabajo grupal. A mis amigos que hice fuera de la carrera, Vito, Pablo, Nacho, quienes se volvieron mi familia en Concepción, compartiendo todo tipo de experiencias. A quienes formaron mi segunda familia en Valdivia, que durante estos años siempre me recibieron con los brazos abiertos.

Aprovecho esta instancia de agradecer a los profesores que estuvieron en mi formación, por lo enseñado dentro y fuera del aula. A Felipe, por motivarme a seguir y desarrollar el área que realmente me gusta en el ámbito profesional, y por ayudarme como un amigo durante este proyecto. A Bernardo un agradecimiento por la paciencia y el apoyo en MMC, además de las reuniones improvisadas donde nunca faltaron las risas.

Un agradecimiento especial a la Pali, que ha sido un apoyo fundamental en todo este proceso y me alegra que sea parte de esta etapa.

Gracias a todos quienes han sido parte de mi vida universitaria.

Resumen

Las motocicletas son sistemas con un comportamiento dinámico complejo que pueden volverse inestables en determinadas condiciones de conducción. Evitar estas inestabilidades desde la fase de diseño no es trivial, ya que dependen de varios parámetros interrelacionados, uno de los cuales es la aerodinámica. Las fuerzas aerodinámicas en un vehículo pueden describirse esencialmente por sus componentes longitudinal (arrastre) y vertical (sustentación) que actúan en un punto conocido como centro de presión (CoP). Además, la fuerza de sustentación, que se ha utilizado de forma importante en las motocicletas deportivas en los últimos años, también puede influir en la estabilidad, sin embargo, su efecto no se ha descrito en la literatura. Por lo tanto, el objetivo de esta investigación es desarrollar un modelo de estabilidad que tenga en cuenta la fuerza de sustentación y las diferentes posiciones del CoP. Para ello, implementamos un modelo básico de estabilidad y lo extendimos para cumplir nuestros requisitos. Consideramos la sustentación aerodinámica creada por las alas invertidas y la posición del CoP. Además, desarrollamos un modelo capaz de considerar condiciones de curvas constantes. El resultado contribuye a la comprensión de la dinámica de la motocicleta y puede servir como aproximación inicial a los estudios de estabilidad de la motocicleta.

Palabras clave – Estabilidad, Aerodinámica, Motocicleta, Modelo.

Abstract

Motorcycles are systems with complex dynamic behaviour that can become unstable under certain driving conditions. Avoiding such instabilities from the design stage is not trivial since they depend on various interrelated parameters, one of which is aerodynamics. Aerodynamic forces in a vehicle can be essentially described by its longitudinal (drag) and vertical (lift) components acting in a point known as the centre of pressure (CoP). Further, the lift force, which has been used importantly in sports motorcycles in recent years, can also influence stability, however, its effect has not been described in the literature. Therefore the aim of this research is to develop a stability model that considers downforce and different CoP positions. To this end, we implemented a basic stability model and extended it to fulfil our requirements. We consider the aerodynamic lift created by the inverted wings and the position of the CoP. Additionally, we developed a model that is capable of considering steady cornering conditions. The result contributes to the understanding of motorcycle dynamics and can serve as an initial approach to motorcycle stability studies.

Keywords – Weave, Wobble, Downforce, Motorcycle stability, Aerodynamics.

Contents

List of Tables

List of Figures

Chapter 1

Introduction

This chapter briefly introduces the problem of motorcycle stability and aerodynamic lift, together with a brief state-of-the-art and the solution proposed. Subsequently, general and specific objectives of this work are presented, followed by the methodology.

1.1 Problem description

Motorcycle racing focuses on the pursuit of better lap times which is achieved by increasing top and cornering speed. To increase top speed, power output needs to be maximised while aerodynamic and mechanic drag are minimised. Conversely, to increase cornering speed, motorcycle grip needs to be maximised, which is achieved by adequately balancing power delivery, suspension settings and aerodynamic forces. Additionally, settings for top speed are usually in conflict with those for cornering. For example, if there is excessive power delivery, tyres suffer premature wear, and grip during cornering decreases. On the other hand, maximising grip increases drag and worsens the top speed. Therefore, it has been seen that the winning motorcycle is the one that finds the best balance between cornering and top speed.

Large racing motorcycles, like the ones used in MotoGP, suffer a phenomenon called understeering due to its Centre of Mass (CoM) being towards the front end (Lot & Sadauckas, 2021). Understeering behaviour means the front axle begins to slip before the rear axle, therefore, the vehicle turns less than desired. On the contrary, oversteering means the rear axle slips more than the front, resulting in a tendency of excessive rotation of the vehicle. Therefore, neutral behaviour is sought, giving a better feeling to the rider

and better vehicle control.

In motorsport, a solution to this problem is the inclusion of the motorcycle's aerodynamic properties in its design. Since the objective is to maximise the lateral force on the wheels, the grip is considered as the resistance of the tyres to lateral slip. When a downforce is added to the front axle, the grip in the front wheels increases, the tendency of "wheelie" reduces and the vehicle becomes oversteering. Similarly, when downforce is added to the rear axle, more grip is generated in the rear tyres and the vehicle becomes understeering. Therefore, for each race, there is an ideal setup, which may not be optimal for other circumstances.

However, the aerodynamic properties of a motorcycle change over the course of a race. The movement of the rider generates air flow interference, changing the aerodynamic effects of some devices. Sport motorcycles have a longer suspension travel compared to sports cars, making their pitch angle constantly change. In conjunction with the previous factors, motorcycles lean for cornering, changing both geometry and airflow through their body. Consequently, the aerodynamics of a motorcycle is constantly changing, making it more challenging to have an ideal vehicle setup.

To simplify the aerodynamic analysis effects are condensed in a single force and moment acting on the Centre of Pressure (CoP). From the literature, it is known that CoP needs to be behind the CoM to keep the system stable (Foale, 2002). But to correct understeering behaviour is sought to have it towards the front end, which may compromise the motorcycle stability.

The study of motorcycle lateral stability encompasses several phenomena, with a primary focus on the crucial modes of vibration, which are Weave and Wobble. The firsr is a low-frequency oscillation, from 0.5 to 5 [Hz], similar to a fishtail movement, while the latter is an oscillatory movement from the motorcycle steering with a frequency between 5 and 10 [Hz]. It has been shown that multiple factors can affect those modes of vibration, such as frame stiffness, and tyre properties, among others. However, there is no clarity about the influence of aerodynamic lift and CoP position on motorcycle stability.

1.2 State of the art

1.2.1 Stability

Motorcycle stability has been a field of study for more than 40 years, the first attempt to predict Weave and Wobble modes was done by Sharp (1971). His mathematical model has four Degrees of Freedom (DoF) which are roll, yaw, steer, and lateral displacement. This paper considers two rigid bodies joined at the steering axis, with a linear steering damper. The work of Sharp (1971) is now a classic model for motorcycle stability studies, being the foundation of several publications.

In the following years, the influence on the stability of certain system components has been studied. Frame flexibility has been proven to affect mainly in weave mode, damping it at medium and high speeds (Sharp (1974); Kane (1979)). Koenen & Pacejka (1982) show the relation between rider lean and *weave* mode, along with the effect of the rotating wheel dampening the *wobble* mode. A detailed tyre model is considered by Cossalter et al. (2002b), where they demonstrated its impact on *weave* and *wobble* modes by considering detailed characteristics of the front tyre. It is clear that several parameters affect stability and considering them all together generates more precise predictions.

A new stability model with 11 DoF is presented by Cossalter & Lot (2002), with more detailed approaches and predictions closer to the real behaviour. It takes into account the motorcycle suspension and the dynamic behaviour of the tyres in combination with its geometric shape. This model is extended, adding a DoF to consider fork bending, showing an important effect over *wobble* mode (Cossalter et al., 2007). All of the detailed considerations bring better results to the model, however, at the same time, make it more complex and difficult to evolve.

Additionally, several other works were done in the motorcycle stability field, testing different models and modifications. For example, Lot & Lio (2004) developed a model to describe the procedures for the automatic generation of the equations of motion. Similarly, Cheli et al. (2006) developed an independent model to study motorcycle stability and compared the results with experimental tests. On the other hand, stability of the motorcycle while cornering was studied by Cossalter et al. (2004), including experimental tests. Finally, all of the mentioned works presents similar plots for stability, within a certain range of values regardless of the numerous considerations, as shown in Figure 1.1.

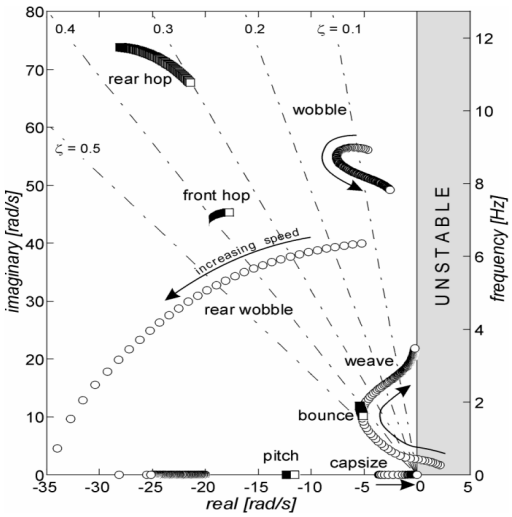

(a) Stability in (Cossalter & Lot, 2002)

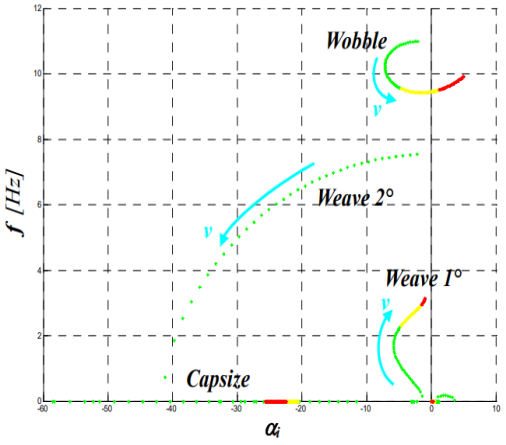

(b) Stability in (Cheli et al., 2006)

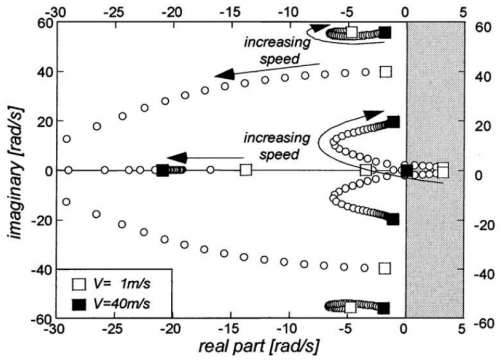

(c) Stability in (Lot & Lio, 2004)

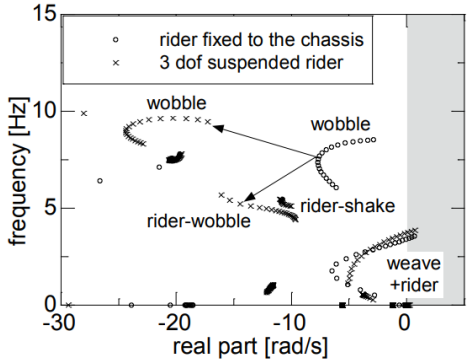

(d) Stability in (Cossalter et al., 2011)

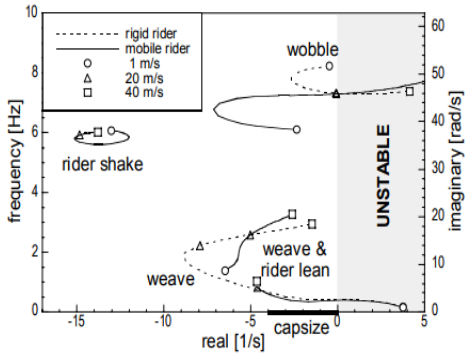

(e) Stability in (Cossalter et al., 2007)

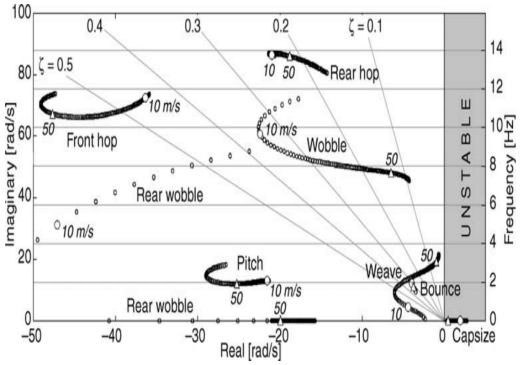

(f) Stability in (Cossalter et al., 2004)

Figure 1.1: Stability plots available on the literature.

1.2.2 Aerodynamics

The influence of aerodynamics on stability was studied under particular cases, understanding the effect of fairings and a top box. Cooper (1983) tested different fairings on a motorcycle and shows an impact only over *wobble* mode because the author can not study *weave*. Furthermore, *weave* mode can be excited by airflow due to some accessories, as it is shown by Bridges & Russell (1987). Aerodynamics can have an important impact on stability, but it was not studied for almost 20 years.

In the 21st century, new research about aerodynamics appears, now centred on airflow around motorcycles. Due to modern trends in sport motorcycling, rider body interference is studied, to understand how it affects airflow through aerodynamic devices, such as winglets (Sedlak et al., 2012). The airflow in inverted wings when cornering is applied to car winglets, showing the importance of considering different flow for cornering conditions (Keogh et al., 2015). Dijck (2015) describes the forces acting on motorcycles when cornering, and it reveals the influence of aerodynamic lift in motorcycle dynamics. Is important to understand the airflow on the motorcycle to study aerodynamics, in particular, the forces generated by them.

Recent research on aerodynamics and stability are an extension of (Cossalter & Lot, 2002) model, a study of a particular motorcycle, and a simple model from a book. The extension of the previously mentioned 11 DoF model shows that adding aerodynamic drag can make the *wobble* mode more damped and the *weave* mode less damped (Meijaard & Popov, 2006). Sharma & Limebeer (2012) presents a complete study about an aerodynamic efficient motorcycle, and includes a study about CoP position using commercial software for motorcycle dynamics. Finally, Lot & Sadauckas (2021) presents a 5 DoF model which considers fork bending, aerodynamic drag and a detailed tyre model. This model is the simplest one that attains reasonable results compared to the literature, which is great for extending its aerodynamic variable.

1.3 Solution proposal

Despite the extensive research on motorcycle stability, there is a potential risk of reaching unstable behaviour when adding aerodynamic forces, which has yet to be studied. To fill that research gap, it is intended to extend Lot & Sadauckas (2021) model, considering longitudinal CoP position and adding aerodynamic lift. This study aims to develop a

motorcycle stability model considering downforce with its respective position. Also, the model has to be suitable for straight running and cornering conditions.

1.4 General objective

Develop a basic mathematical model to study motorcycle stability considering downforce and different centre of pressure positions in straight-running and steady cornering.

1.5 Specific objectives

1. Estimate geometrical characteristics of inverted wings used in sports motorcycles to obtain a range of aerodynamic forces.
2. Develop a motorcycle stability model based on Lot & Sadauckas (2021) including downforce and changing centre of pressure position.
3. Develop equations of motion to study motorcycle stability in steady cornering considering downforce and changing centre of pressure position.

1.6 Methodology

Estimate geometrical characteristics of inverted wings used in sports motorcycles.

In motorsport, inverted wings create downforce and modify vehicle behaviour as mentioned earlier. Since there are different circumstances in each race, aerodynamic devices vary from one to another. Therefore, it is desired to know how are the main wing profiles used in sports motorcycles and understand their characteristics. First, a literature review about wings will be done, to understand how they generate lift and their defining parameters. Then, from literature and motorsport information available on the web, characteristics of typical wing geometries will be extracted.

Develop a motorcycle stability model for straight running conditions.

To develop a stability model with lift and CoP position, the model of Lot & Sadauckas (2021) will be extended. The first step will be to set the CoP position with x (longitudinal) and z (vertical) values. Then, aerodynamic components will be included in load transfer

over normal forces. Moreover, equations of motion will be modified, including downforce in the vertical axis.

Develop a motorcycle stability model for steady turning conditions.

The first model developed in this work is suited for straight-running conditions, which means several assumptions and linearisations. Then, to study the behaviour in steady cornering conditions it is necessary to modify some components. In particular, the main DoF affected is the roll of the motorcycle, now considering a base lean angle plus the oscillation. Additionally, wheel spin velocity, and steering angle are sensitive to cornering conditions Therefore, equations of motion are modified and generalised.

Work plan

Result	Task	Week 1	2	3	4	5	6	7	8	9	10	11	12	13	14	15	16	17
	1. Definir objectives and methodology																	
Estimate geometrical characteristics	1. Examine pictures of 2023 MotoGP																	
	2. Study aerodynamic theory																	
	3. Estimate aerodynamic characteristics																	
	4. Determine speed dependent equations																	
Develop model for straight running conditions	1. Examine Lot & Sadauckas 2021 model																	
	2. Set longitudinal position of the CoP																	
	3. Modify normal forces																	
	4. Modify equations of motion																	
Develop model for steady cornering conditions	1. Examine roll-sensitive components																	
	2. Define new parameters																	
	3. Modify equations of motion																	
	4. Write final report																	

Figure 1.2: Gantt chart of the project

Summarising, the present work has three main stages, where the first is the study about motorcycle wings. Secondly, the first modification to the original model is done, including downforce with a longitudinal position. Finally, the model is modified again for a more generalised case that allows to consider an initial roll angle for cornering.

Chapter 2

Aerodynamics

This chapter formally presents the two main topics covered in the present work: Stability and Aerodynamics. First, the fundamentals of stability analysis are presented. Then, a brief review of motorcycle aerodynamics and a characterisation of winglets used in sports motorcycles is described.

2.1 Stability

Stability can be defined as the capacity of a system to return to its equilibrium state after a perturbation. Modes of vibration are distinct patterns of motion that a system can adopt when excited from its equilibrium position. A stable system remains within predefined bounds and is essential for reliable and predictable operation. Each mode corresponds to a unique frequency and represents a combination of displacements and velocities of the components of the system. On the other hand, resonance is when an external force is applied at or near the natural frequency of the system, resulting in a heightened response amplitude. Resonance can lead to significant magnification of vibrations, causing potential performance issues. Understanding stability, modes of vibration, and the potential for resonance is crucial in engineering design, as it ensures safe and efficient systems for a wide range of uses.

To study the stability of a system, equations of motion are formulated and the associated eigenvalues problem is solved. The general eigenvalue problem reads

$$\mathbf{A}\mathbf{u} = s\mathbf{u}, \tag{2.1}$$

where **A** is the matrix of the system made from equations of motion (EoM), **u** is the matrix of eigenvectors and s are the eigenvalues. If eigenvalues are complex, means that the system oscillates. If the real part of the eigenvalues is negative, the system is stable. Summarising, the study of the stability of a system consists in solving the associated eigenvalue problem and relating it to the modes of vibration.

2.2 Aerodynamics

The aerodynamics of motorcycles is challenging to study due to their irregular shape and constantly changing conditions. For several years, the main goal of aerodynamic studies on motorcycles relied on the search for a lower drag coefficient. However, nowadays racing teams are using aerodynamic downforce to enhance the performance of motorcycles.

History of motorcycle aerodynamics

At the beginning of aerodynamic studies of racing motorcycles, the main strategy was to reduce the drag force to increase top speed. Large fairings used in early racing motorcycles were a solution to the problem (see Figure 2.1a). However, those fairings had a large lateral area, which caused instabilities when exposed to cross-winds. Therefore, safety regulations prohibited it and next generations fairings were considerably smaller as can be seen in Figure 2.1b. This fairing shape continued its progressive evolution for almost six decades as shown in Figure 2.2, until the new aero-fairings appeared in 2018 changing the scene.

The main purpose of the latest aero-fairings is to take advantage of downforce. Frontal downforce is used to decrease the tendency of "wheelie" in straight line and to enhance the cornering grip. While rear downforce is used to decrease the tendency of "stoppie" at braking. *"Wheelie"* is the phenomenon where the front wheel loses contact with the ground due to excessive load transfer to the rear wheel in acceleration. On the contrary, *"stoppie"* is the phenomenon where the rear wheel losses contact with the ground due to excessive load transfer to the front wheel while braking. In recent motorcycle races, both phenomena have seriously decreased in comparison with past years.

As can be seen in Figure 2.3, downforce in motorcycles is not something new, Suzuki experimented with a primitive winglet in 1979 with the RG 500. However, for some undocumented reasons, these experiments stopped and winglets were not part of the new MotoGP era until Ducati used it in 2009 (Sedlak et al., 2012) (see Figure 2.4a). Furthermore,

(a) 1955 Moto-Guzzi v8 (Cathcart, 2013).

(b) 1966 Honda RC166 (Shea, 2018).

Figure 2.1: Early motorcycle fairings.

in 2015, Ducati was the first manufacturer to include winglets in its prototype, as shown in Figure 2.4b, which became a tendency among all makers. Nevertheless, the new aerodynamic devices lasted until 2017 when were banned due to safety reasons, giving way to the current aero-fairings. Aero-fairings focuses on increasing overall vehicle performance through downforce usage and airflow distribution.

Winglet characterisation

The key part of aero-fairings, and the most relevant to the present work, are the inverted wings used in the front of the motorcycle (Figure 2.5). Those inverted wings are different among manufacturers, however, the average properties can be deduced from images found in the web. The main characteristics of inverted wings are the airfoil, the surface area and the angle of attack. Since in the present work wings will be considered perfectly rigid and the model does not consider pitch degree of freedom, the angle of attack will be constant. Whereas the airfoil is used to determine the lift coefficient (C_l) and the airfoil-induced drag coefficient (C_d) range.

Lifting line theory

Since each racing team uses different airfoils and there is no public information available about wings used, is it necessary to estimate some parameters. Here, the main variable is the C_l, however, to have a reasonable approach to a real airfoil, a simple theory is used. First, the basic theory to estimate C_l from an airfoil is called "*Thin Airfoil theory*", and its equation is $C_{l\alpha} = 2\pi\alpha$, where α is the angle of attack. However, this theory considers an infinite wingspan and does not provide a C_d. Secondly, another basic theory is called

(a) 1979 Suzuki RG500.

(b) 1985 Honda NSR500 (Scott, 2019).

(c) 1996 Honda NSR500 (Repsol, 2023).

(d) 2008 Ducati Desmosedici (Scott, 2008).

Figure 2.2: MotoGP fairings in each decade.

"*Lifting Line Theory*" (LLT), which simplified theory for symmetrical airfoils and depends on the wing aspect ratio (AR). LLT attains reasonable results compared to reality, thus, is an acceptable approach for this work. Furthermore, LLT is used to estimate the ranges of lift and drag forces generated by each wing considering several angles of attack and surfaces. Finally, the equation for the lift coefficient is

$$C_l = C_{l\alpha}\frac{AR}{AR+2}, \tag{2.2}$$

where AR is given by the expression $AR = \frac{wingspan}{chord}$, considering the wingspan of a single wing. It is useful to mention that the wingspan is the distance from the wing base in the motorcycle fairing to its tip. While chord is the distance from the front end to the rear end of the wing.

The LLT equation for airfoil-induced drag coefficient is

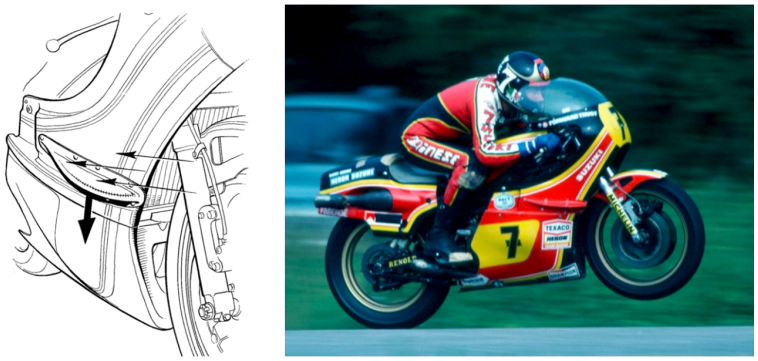

Figure 2.3: Winglet used in 1979 Suzuki RG500 (Foale, 2002).

$$C_d = C_{d0} + \frac{C_l^2}{e\pi AR}, \tag{2.3}$$

where e is the Oswald efficiency number, and C_{d0} is the minimum drag coefficient (Scott, 2004).

Now the equation for downforce is

$$D = \frac{1}{2}\rho C_l S V^2, \tag{2.4}$$

where ρ is the air density, V is the longitudinal speed and S is the projected surface area of the wing.

Then, the drag force is calculated by

$$F_{ad} = \frac{1}{2}\rho C_d S V^2, \tag{2.5}$$

which is the classical formula to obtain the drag force generated by a body.

Results

All characteristics are based on what has been seen in the 2023 MotoGP championship. Pictures of 2023 MotoGP bikes are shown in Figure 2.5

- **Surface**: *Fédération Internationale de Motocyclisme* (FIM) regulations set the maximum width of the fairing to 600 [mm]. Therefore, by dividing this magnitude into three: two wings and the central part of the fairing, the maximum length of

each wing could be 200 [mm]. Whereas, by a visual inspection of several pictures of MotoGP motorcycles, the chord is set to 100 [mm] to keep the aspect ratio.

- **Number of wings**: Ducati motorcycles use four double main wings at the front. Whereas, Aprilia, Honda, KTM, and Yamaha use only two double main wings in the front. Yamaha in some races uses an extra wing at the tail of the motorcycle, as well as KTM and Aprilia. On the contrary, Ducati and Honda use smaller diagonal wings, which do not create downforce and their effect is beyond the scope of the present study. To sum up, four wings at the front end and one at the rear end are considered to generate downforce.

- **Lift coefficient**: Considering an angle of attack of 15°, LLT gives a maximum C_l of 1.6. Alternatively, other studies about the aerodynamics of motorcycles consider NACA airfoils. Kamalakkannan et al. (2020) uses NACA 0012 and Pednekar (2021) uses NACA 6412, which information can be seen in Table 2.1 Finally, the range of C_l used is from - 0.5 to 1.7, since a motorcycle without wings generates lift and wings generates downforce.

Airfoil	α	C_l	C_d	**Chord**	**Length**	**N° Wings**	**Total Lift [N]**
0012	10	1.2	0.01	0.1	0.2	5	595
6412	10	1.95	0.015	0.1	0.2	5	967
LLT	10	1.09	0.288	0.1	0.2	5	540
LLT	15	1.64	0.63	0.1	0.2	5	813
LLT	20	2.2	1.1	0.1	0.2	8	1746

Table 2.1: Airfoil data

XFOIL analysis

To verify the values used for lift coefficients, the specialised software XFOIL is used. XFOIL is a relatively simple tool for design and analysis of subsonic airfoils with a database of four and five digit NACA profiles. Therefore, the NACA airfoils previously mentioned were tested in the software, obtaining the values showed in the Table 2.1.

Summarising, stability is a challenging field of study with multiple ways to understand its results, however, with the right techniques the work is more efficient. Besides that, it is really important to understand the characteristics of the winglets, since they produce a force that excites the system, affecting its stability. Furthermore, it was seen that motorcycle aerodynamics had encompassed several objectives throughout its history.

(a) 2009 Valentino Rossi's Ducati Desmosedici (Sedlak et al., 2012).

(b) 2016 Andrea Dovizioso's Ducati Desmosedici (Beeler, 2018).

Figure 2.4: First winglets in modern era.

(a) 2023 Alex Marquez's Ducati Desmosedici (Iwanbanaran, 2023).

(b) 2023 Fabio Quartararo's Yamaha YZR-M1 (McLaren, 2023).

(c) 2023 Maverick Viñales' Aprilia RSGP (Fialho, 2023).

(d) 2023 Brad Binder's KTM RC16 (Ramanujam, 2023).

Figure 2.5: 2023 MotoGP motorcycles.

Chapter 3

Straight running

This chapter presents the original stability model extracted from Lot & Sadauckas (2021) and the modifications to include aerodynamic lift with longitudinal position.

3.1 Original model

The present work is an extension of the previously mentioned model. The main goal of the model is to predict the stability of the two well-known modes of vibration: *Weave* and *Wobble*. System equations are developed, which include the sum of forces and moments of the whole vehicle in x, y and z axis. Moments with respect to the bending axis of the fork (β), respect to the steering (δ), and a linear tyre model are considered. This model has five DoF, being the simplest one with reasonable results according to Lot & Sadauckas (2021). The DoF are roll (φ), yaw (ψ), steer angle (δ), fork bending (β) and lateral velocity of the chassis (V_y). Furthermore, Lot & Sadauckas (2021) presents equations of motion (EoM) and the state-space formulation matrices.

3.1.1 Model geometry

The model represents the motorcycle as a system composed of four bodies: a rear frame (chassis, engine, rider and tank), a front frame (fork and handlebar) and two wheels. The front and rear frames are connected by the steering axis as a revolute joint, as well as the wheels with the frames. The rider is considered rigidly attached to the rear frame of the motorcycle. The motion of the suspension is not taken into account, therefore, the pitch angle is negligible.

There are two coordinate systems: The main coordinate system and the front coordinate system. The main coordinate system has its origin $\boldsymbol{O}$ at the contact point of the rear wheel $\mathbf{C}_r$. The x and y axes lie permanently in the road plane, while the z axis is perpendicular to the ground and is directed downwards. The front coordinate system, which is used for the front frame and the bending body, has its origin in the joint of the rear and front frames. Thus, its z axis is rotated at an ε angle from the main system, remaining aligned with the steering axis. The lateral and longitudinal forces of the ground exerted on the tyres are always on the road plane, whereas normal force is parallel to the z axis.

In Figure 3.1 the overall geometry can be seen to understand the principal dimensions. Additionally, in Figure 3.2 is presented a detailed view of the front frame.

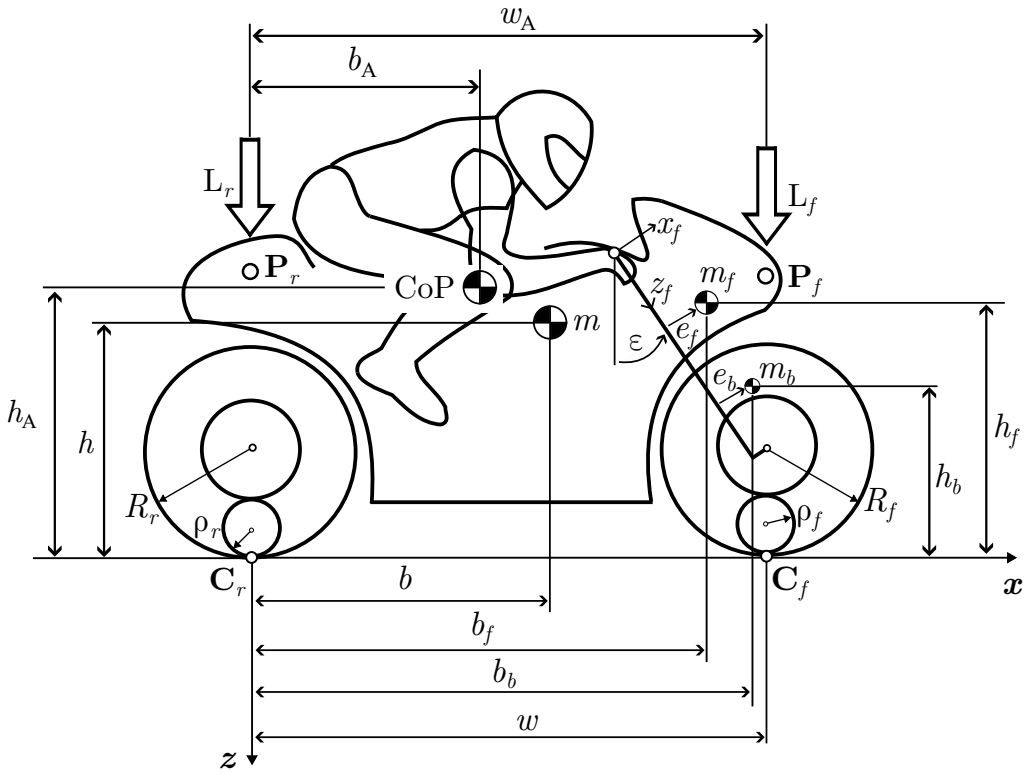

Figure 3.1: Geometry of the model, modified from Lot & Sadauckas (2021).

3.2 Kinematic equations

Since motorcycles roll in cornering, and the fork is installed with a caster angle ε, it is necessary to establish some kinematical relations.

The front wheel roll φ_f differs from roll measured at the chassis φ and are related by

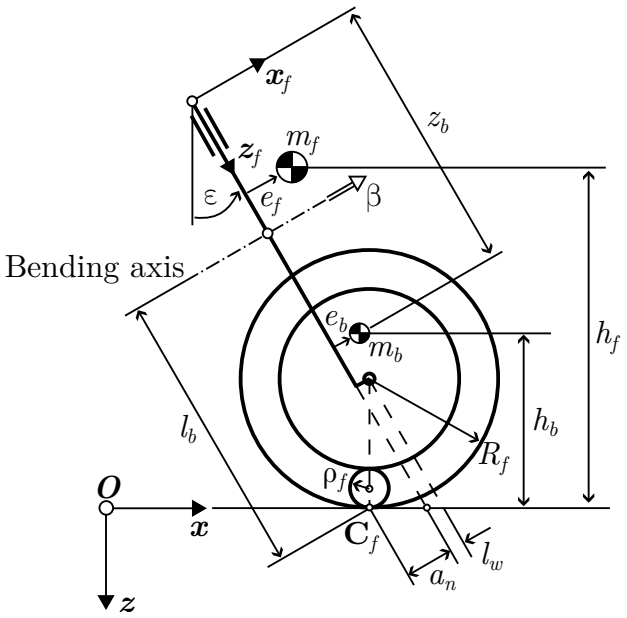

Figure 3.2: Front frame geometry.

$$\varphi_f = \varphi + \delta \sin(\varepsilon) + \beta \cos(\varepsilon), \tag{3.1}$$

Similarly, the angle between the symmetry axis of the chassis and the front wheel projected to the ground Δ is different to δ, so the relation is

$$\Delta = \delta \cos(\varepsilon) - \beta \sin(\varepsilon). \tag{3.2}$$

Regarding the angular velocity of the front and rear wheels, ω_f and ω_r respectively, they are defined as

$$\omega_r = \frac{V_x}{R_r} \tag{3.3a}$$

$$\omega_f = \frac{V_x}{R_f}. \tag{3.3b}$$

Next, some other geometrical parameters are used in equations of motion, where b_f and b_b are the longitudinal position of the front assembly CoM and the bending mass CoM, respectively. Additionally, z_b is the vertical position of bending mass CoM in the front coordinate system. Then, their equations are

$$b_f = w + \frac{x_f + a_n - h_f \sin(\varepsilon)}{\cos(\varepsilon)} \tag{3.4a}$$

$$b_b = w + \frac{x_b + a_n - h_b \sin(\varepsilon)}{\cos(\varepsilon)} \tag{3.4b}$$

$$z_b = l_b + \frac{(a_n + x_b)\sin(\varepsilon) - h_b}{\cos(\varepsilon)}. \tag{3.4c}$$

Lastly, the practical sideslip of the motorcycle tyres is expressed as

$$\alpha_r = -\frac{V_y}{V_x} \tag{3.5a}$$

$$\alpha_f = \delta\cos(\varepsilon) - \beta\sin(\varepsilon) + \frac{a_n\dot{\delta} - w\dot{\psi} - V_y + (l_b - \rho_f\cos(\varepsilon))\dot{\beta}}{V_x}. \tag{3.5b}$$

3.2.1 Forces description

First, α' is the tyre contact patch sideslip and γ is the wheel camber, which we represent as φ since is the same as roll angle. Second, k_a and k_t are the normalised stiffness of aligning and twist torque respectively. At last, k_α and k_γ are the normalised sideslip and camber stiffness respectively.

Lateral forces in both tyres are considered linear and are calculated as follows

$$Y_r = (k_{\alpha r}\alpha'_r + k_{\gamma r}\varphi_r)N_r \tag{3.6a}$$

$$Y_f = (k_{\alpha f}\alpha'_f + k_{\gamma f}\varphi_f)N_f, \tag{3.6b}$$

where N_f and N_r are the normal forces on the front and rear wheels. Then, including load transfer due to aerodynamic drag, inertial forces and torques of the spinning wheels, it results

$$N_r = N_{r0} + \frac{h_A}{w}F_{ad} + \frac{1}{w}\left(mh + \frac{I_{\omega r}}{R_r} + \frac{I_{\omega f}}{R_f}\right)a_x \tag{3.7a}$$

$$N_f = N_{f0} - \frac{h_A}{w}F_{ad} - \frac{1}{w}\left(mh + \frac{I_{\omega r}}{R_r} + \frac{I_{\omega f}}{R_f}\right)a_x. \tag{3.7b}$$

For static loads, the normal forces are

$$N_{r0} = \left(1 - \frac{b}{w}\right) mg$$

$$N_{f0} = \frac{b}{w} mg.$$

Following the formulation proposed by Lot & Sadauckas (2021), tyre yaw torques for front and rear tyres can be calculated as

$$M_{rz} = (k_{ar}\alpha'_r + k_{tr}\varphi_r)N_r \tag{3.9a}$$

$$M_{fz} = (k_{af}\alpha'_f + k_{tf}\varphi_f)N_f, \tag{3.9b}$$

where k_a and k_t are the normalised stiffness of aligning and twist torque respectively.

Aerodynamic drag force for the entire motorcycle is given by

$$F_{ad} = \frac{1}{2}\rho C_D A V_x^2, \tag{3.10}$$

where A is the frontal area of the motorcycle.

Tyre transient behaviour model considers relaxation lengths, which depend on normal forces and are given by

$$L_r = \frac{k_{\alpha r} N_r}{k_{lr}} \tag{3.11a}$$

$$L_f = \frac{k_{\alpha f} N_f}{k_{lf}}, \tag{3.11b}$$

where k_{lf} and k_{lr} are the transverse stiffness of the front and rear tyre respectively.

3.3 Equations of motion

In the original text (Lot & Sadauckas, 2021), the EoMs were derived with MAPLE software. However, the EoMs were revised and derived by the author (Gonzalez, 2023), using Python and SymPy due to the accessibility of the software.

3.3.1 Forces

The sum of forces can be assessed as

$$m\mathbf{a} + m_f\mathbf{a_f} + m_b\mathbf{a_b} = \mathbf{f_r} + \mathbf{f_f} + \mathbf{f_A}. \tag{3.12}$$

Then, expressing the terms of the equations along each axis of the main coordinate system it reads

$$ma_x = X_r + X_f - F_{ad} \tag{3.13a}$$

$$m(\dot{V}_y + b\ddot{\psi} + h\ddot{\varphi} + V_x\dot{\psi}) + m_f e_f\ddot{\delta} - m_b z_b\ddot{\beta} = Y_r + Y_f + (\delta\cos(\varepsilon) - \beta\sin(\varepsilon))X_f \tag{3.13b}$$

$$0 = -mg - (N_f + N_r), \tag{3.13c}$$

where a_x is the longitudinal acceleration, and X_r is the rear wheel traction force. Additionally, X_f is the longitudinal force of the front wheel, which is considered 0 in this work due to the inexistent traction or brake forces. b and h are the longitudinal and vertical motorcycle CoM position, respectively. Similarly, e_f is the longitudinal position of the front assembly CoM in the front coordinate system.

3.3.2 Moments

The rotational EoMs with respect to the origin of the main coordinate system, which is aligned with the rear wheel contact point $\mathbf{C}_r$ are expressed as

$$\mathbf{I^o}\dot{\omega} + \mathbf{I_f^o}\dot{\omega_f} + \mathbf{I_b^o}\dot{\omega_b} + \omega \times \mathbf{I^o}\omega + \omega_\mathbf{f} \times \mathbf{I_f^o}\omega_\mathbf{f} + \omega_\mathbf{b} \times \mathbf{I_b^o}\omega_\mathbf{b} = M_x + M_y + M_z \tag{3.14}$$

Inertias

Since the inertias of the different bodies is expressed on their centre of mass, it is necessary to transfer them to the origin point $\boldsymbol{O}$ of the main system. First, we use Steiner's theorem for moments of inertia (MoI), which states that $I_{ii} = I_{CoM} + md^2$. Along with that, we use also the product of inertia (PoI), defined as $I_{ij} = I_{x'z'} + mxy$ As a result, the inertias of the different bodies are now expressed in the origin of their respective coordinate systems. Thus, it is easier to work and understand the inertias of the motorcycle.

Along with that, the front coordinate system needs to be rotated at an angle of ε to be aligned with the main system as explained on Shames (1999). Below we include a brief example of the rotation, where a_{ki} and a_{qi} are the direction cosines.

First, for MoI, the transformation is given by

$$\begin{aligned} I_{kk} =& I_{xx}a_{kx}^2 - I_{xy}a_{kx}a_{ky} - I_{xz}a_{kx}a_{kz} \\ & - I_{xy}a_{ky}a_{kx} + I_{yy}a_{ky}^2 - I_{yz}a_{ky}a_{kz} \\ & - I_{xz}a_{kz}a_{kx} - I_{yz}a_{kz}a_{ky} + I_{zz}a_{kz}^2. \end{aligned} \tag{3.15}$$

Then, the transformation for PoI is

$$\begin{aligned} -I_{kq} =& I_{xx}a_{kx}a_{qx} - I_{xy}a_{kx}a_{qy} - I_{xz}a_{kx}a_{qz} \\ & - I_{xy}a_{ky}a_{qx} + I_{yy}a_{ky}a_{qy} - I_{yz}a_{ky}a_{qz} \\ & - I_{xz}a_{kz}a_{qx} - I_{yz}a_{kz}a_{qy} + I_{zz}a_{kz}a_{qz}, \end{aligned} \tag{3.16}$$

Finally, by applying it to the reference frame of the front assembly, it results

$$\begin{aligned} a_{x'x} &= \cos(\varepsilon) \\ a_{x'y} &= 0 \\ a_{x'z} &= \cos(90 - \varepsilon) = \sin(\varepsilon) \end{aligned}$$

$$\begin{aligned} a_{z'x} &= \cos(90 + \varepsilon) = -\sin(\varepsilon) \\ a_{z'y} &= 0 \\ a_{z'z} &= \cos(\varepsilon), \end{aligned}$$

where x' and z' are the target axis, in this case, the body reference frame, while x, y and z are the axis fixed to the front assembly.

Now, we present the extended form of the equations. Due to the its length, they are split into two: the inertial side and the external moments side.

Thus, the inertial side of the sum of moments is

$$(mbh - I_{xz})\ddot{\psi} + (mh^2 + I_{xx})\ddot{\varphi} + (m_f e_f h_f + I_{fzz}\sin(\varepsilon))\ddot{\delta} + (I_{bxx}\cos(\varepsilon) - m_b h_b z_b)\ddot{\beta} + mh(\dot{V}_y + V_x\dot{\psi}) = M_x \quad (3.17a)$$

$$-mha_x - (I_{\omega f}\dot{\omega}_f + I_{\omega r}\dot{\omega}_r) = M_y \quad (3.17b)$$

$$(mb^2 + I_{zz})\ddot{\psi} + (mbh - I_{xz})\ddot{\varphi} + (m_f e_f b_f + I_{fzz}\cos(\varepsilon))\ddot{\delta} + (I_{bxx}\sin(\varepsilon) - m_b b_b z_b)\ddot{\beta} + mb(\dot{V}_y + V_x\dot{\psi}) + (m_b z_b\beta - mh\varphi - m_f e_f\delta)\dot{V}_x - I_{\omega r}(\omega_r\dot{\varphi} + \dot{\omega}_r\varphi) - I_{\omega f}(\omega_f\dot{\varphi}_f + \dot{\omega}_f\varphi_f) = M_z, \quad (3.17c)$$

While the side of external moments of the equations is presented below

$$M_x = [(a_n - \sin(\varepsilon)\rho_f)\delta + (l_b - \cos(\varepsilon)\rho_f)\beta - \rho_f\varphi]N_f - \rho_r\varphi N_r + mgh\varphi - m_b g z_b\beta + m_f g e_f\delta \quad (3.18a)$$

$$M_y = wN_f - bmg + h_A F_{ad} \quad (3.18b)$$

$$M_z = wY_f - \rho_r X_r\varphi + h_A F_{ad}\varphi + M_{rz} + M_{fz} + [(a_n + \omega\cos(\varepsilon) - \rho_f\sin(\varepsilon))\delta - \rho_f\varphi + (l_b - \rho_f\cos(\varepsilon) - w\sin(\varepsilon))\beta]X_f, \quad (3.18c)$$

3.3.2.1 Moments with respect to the steering axis δ

The steering axis is aligned with the z axis of the front reference frame, which means that inertias has to be translated and rotated to the steering axis. Then, its behaviour is governed by the following equation

$$(m_f e_f^2 + I_{fzz})\ddot{\delta} + (m_f e_f h_f + I_{fzz}\sin(\varepsilon))\ddot{\varphi} - m_b e_b z_b \ddot{\beta} + (m_f e_f b_f + I_{fzz}\cos(\varepsilon))\ddot{\psi} + \\ m_f e_f(\dot{V}_y + V_x\dot{\psi} + \dot{V}_x\cos(\varepsilon)\delta) + I_{\omega f}\omega_f(\dot{\psi}\sin(\varepsilon) - \dot{\varphi}\cos(\varepsilon)) - I_{\omega f}(\omega_f\dot{\beta} + \dot{\omega}_f\beta) = \\ M_\delta - c_\delta\dot{\delta} - a_n Y_f + M_{fz}\cos(\varepsilon) + [(l_b\cos(\varepsilon) + a_n\sin(\varepsilon))\beta + \rho_f\cos(\varepsilon)\varphi_f]X_f + \\ + [(a_n - \rho_f\sin(\varepsilon))\varphi_f + (l_b\sin(\varepsilon) + a_n\cos(\varepsilon))\beta]N_f + \\ + (a_x\cos(\varepsilon) + g\sin(\varepsilon))(m_f e_f\delta - m_b z_b\beta) + g m_f e_f\varphi, \quad (3.19)$$

where M_δ is the rider input torque, and c_δ is the torque generated by steering bearings friction and the action of and steering damper if it exists.

3.3.2.2 Fork bending

One of the main contributions of Lot & Sadauckas (2021) model, is the lateral fork bending. The importance of considering fork bending is demonstrated in Cossalter et al. (2007). In this case, fork bending angle is presented as β, and acts in the bending axis, which is parallel to x axis of the front coordinate system. Then, equation of fork bending oscillation is

$$-(m_b b_b z_b - I_{bxx}\sin(\varepsilon))\ddot{\psi} + (I_{bxx}\cos(\varepsilon) - m_b h_b z_b)\ddot{\varphi} - m_b e_b z_b\ddot{\delta} + \\ + (m_b z_b^2 + I_{bzz})\ddot{\beta} - m_b z_b(\dot{V}_y + V_x\dot{\psi}) + I_{\omega f}\omega_f(\dot{\varphi}_f + \dot{\psi}\cos(\varepsilon)) = \\ - l_b Y_f - M_{fz}\sin(\varepsilon) + [(l_b - \rho_f\cos(\varepsilon))N_f + \rho_f\sin(\varepsilon)X_f]\varphi_f \\ - k_\beta\beta + m_b z_b[a_x(\beta\sin(\varepsilon) - \delta\cos(\varepsilon)) - g\varphi_f], \quad (3.20)$$

where right-hand terms are moments generated with respect to the bending axis x_b. And k_β is the bending stiffness of the fork.

Tyre model

As mentioned at the beginning of the section, the present work uses a model that captures the transient behaviour of the tyres. Since the contact patch of the tyre changes as a consequence of motorcycle roll, its sideslip is affected, generating the new component α'.

The relation between both sideslips is expressed by

$$L_r \frac{\dot{\alpha_r}'}{V_x} + \alpha_r' = \alpha_r + \frac{(1 - k_{\gamma r}) N_r}{k_{lr}} \frac{\dot{\varphi}_r}{V_x}$$
$$L_f \frac{\dot{\alpha_f}'}{V_x} + \alpha_f' = \alpha_f + \frac{(1 - k_{\gamma f}) N_f}{k_{lf}} \frac{\dot{\varphi}_f}{V_x},$$

3.4 Model upgrade

In this section, modifications to the original model are explained, and the new terms in equations are shown underlined to highlight the difference. As mentioned earlier, downforce is calculated through the classical lift equation, depending on the C_l. Since airfoils also generate drag, the equation of aerodynamic drag gets modified and it reads

$$F_{ad} = \frac{1}{2} \rho (C_D A + C_d S) V_x^2, \tag{3.22}$$

where C_D is the motorcycle drag coefficient without airfoils and C_d is the airfoil-generated drag coefficient. Moreover, the CoP position is determined by weighing the front and rear total lift surface areas.

Centre of pressure position

To determine CoP longitudinal position it is necessary to introduce the new length between the position of the front and rear wings. Since it is analogous to the wheelbase w, we define it as w_A. Likewise, the longitudinal position of CoM b is equivalent to the longitudinal position of CoP b_A. Therefore, the equation is

$$b_A = \frac{D_f w_A}{D}, \tag{3.23}$$

where D is the total downforce on the motorcycle and D_f is the downforce generated by the front wings. To avoid introducing more complex parameters, the rear point of the downforce application is considered aligned with $\mathbf{C}_r$.

Normal forces

Since downforce is downwards it increases the normal forces, thus, the resultant forces can be calculated as

$$N_r = N_{r0} + \frac{h_A}{w}F_{ad} + \frac{1}{w}(mh + \frac{I_{\omega r}}{R_r} + \frac{I_{\omega f}}{R_f})a_x + \underline{\left(1 - \frac{b_A}{w_A}\right)D} \tag{3.24a}$$

$$N_f = N_{f0} - \frac{h_A}{w}F_{ad} - \frac{1}{w}(mh + \frac{I_{\omega r}}{R_r} + \frac{I_{\omega f}}{R_f})a_x + \underline{\frac{b_A}{w_A}D}. \tag{3.24b}$$

Equations of motion

Then, EoMs are modified to include downforce in the sum of forces and in the sum of moments. For the sum of forces in the z axis the equation reads

$$0 = -mg - (N_f + N_r)\underline{+D}. \tag{3.25}$$

Besides, external moments in y and z are affected by downforce resulting

$$M_y = wN_f - bmg + h_A F_{ad}\underline{-b_A D} \tag{3.26a}$$

$$M_z = wY_f - \rho_r X_r \varphi + h_A F_{ad}\varphi + M_{rz} + M_{fz} + [(a_n + \omega\cos(\varepsilon) - \rho_f \sin(\varepsilon))\delta - \rho_f\varphi + (l_b - \rho_f\cos(\varepsilon) - w\sin(\varepsilon))\beta]X_f\underline{-b_A D\varphi}, \tag{3.26b}$$

Lastly, all aerodynamic parameters used in the model are detailed in the Table 3.1.

3.4.1 State-space formulation matrices

As mentioned above, the stability of a system can be assessed by solving the eigenvalues problem associated with the system of equations. Here, the system of equations is given by

$$\mathbf{E}\dot{\mathbf{x}} = \mathbf{A}\mathbf{x} \tag{3.27}$$

Where $\mathbf{A}$ and $\mathbf{E}$ are 10x10 matrices, and $\mathbf{x}$ is the 10-dimensional state vector shown below

Parameter	Value	Unit	Description
Wingspan	0.2	m	y axis wing length
Chord	0.1	m	x axis wing length
N° wings	5	-	Number of wings on the motorcycle
C_l	1.5	-	Lift coefficient
$C_D A$	0.467	m^2	Aerodynamic drag factor w/frontal area
w_l	1.448	m	Aerobase
b_l	1.16	m	CoP longitudinal position
h_A	0.35	m	CoP vertical position
e	0.8	-	Oswald efficiency number

Table 3.1: Aerodynamic parameters.

$$\mathbf{x} = \begin{bmatrix} V_y & \dot{\psi} & \dot{\varphi} & \dot{\delta} & \dot{\beta} & \alpha'_r & \alpha'_f & \varphi & \delta & \beta \end{bmatrix}^T \tag{3.28}$$

Therefore, the associated eigenvalues problem is given by

$$\mathbf{A}\,\mathbf{u} = s\,\mathbf{E}\,\mathbf{u} \tag{3.29}$$

Re-written it reads

$$\mathbf{E}^{-1}\,\mathbf{A}\,\mathbf{u} = s\,\mathbf{u} \tag{3.30}$$

Now, the matrices **A** and **E** are presented by their entries due to the extension of their equations.

A matrix is more complicated and depends on longitudinal speed V_x.

$A_{1,2} = -mV_x$

$A_{1,6} = k_{\alpha r} N_r$

$A_{1,7} = k_{\alpha f} N_f$

$A_{1,8} = k_{\gamma f} N_f + k_{\gamma r} N_r$

$A_{1,9} = X_f \cos(\varepsilon) + N_f k_{\gamma f} \sin(\varepsilon)$

$A_{1,10} = -X_f \sin(\varepsilon) + N_f k_{\gamma f} \cos(\varepsilon)$

$A_{2,2} = -mbV_x$

$$A_{2,3} = I_{\omega f}\omega_f + I_{\omega r}\omega_r$$

$$A_{2,4} = I_{\omega f}\omega_f \sin(\varepsilon)$$

$$A_{2,5} = I_{\omega f}\omega_f \cos(\varepsilon)$$

$$A_{2,6} = N_r k_{ar}$$

$$A_{2,7} = N_f k_{af} + N_f k_{\alpha f} w$$

$$A_{2,8} = F_{ad}h_A + I_{\omega f}\dot{\omega}_f + I_{\omega r}\dot{\omega}_r + N_f\left(k_{\gamma f}w + k_{tf}\right) + N_r k_{tr} - X_f\rho_f - X_r\rho_r + a_x hm \underline{- Db_A}$$

$$A_{2,9} = I_{\omega f}\dot{\omega}_f \sin(\varepsilon) + N_f k_{tf}\sin(\varepsilon) + X_f\left(a_n - \rho_f\sin(\varepsilon) + w\cos(\varepsilon)\right) + a_x e_f m_f + N_f k_{\gamma f} w\sin(\varepsilon)$$

$$A_{2,10} = I_{\omega f}\dot{\omega}_f \cos(\varepsilon) + N_f k_{tf}\cos(\varepsilon) + X_f\left(l_b - \rho_f\cos(\varepsilon) - w\sin(\varepsilon)\right) - a_x m_b z_b + N_f k_{\gamma f} w\cos(\varepsilon)$$

$$A_{3,2} = -I_{\omega f}\omega_f - I_{\omega r}\omega_r - V_x hm$$

$$A_{3,4} = -I_{\omega f}\omega_f \cos(\varepsilon)$$

$$A_{3,5} = I_{\omega f}\omega_f \sin(\varepsilon)$$

$$A_{3,8} = -N_f\rho_f - N_r\rho_r + ghm$$

$$A_{3,9} = -I_{\omega f}\dot{\omega}_f \cos(\varepsilon) + N_f\left(a_n - \rho_f\sin(\varepsilon)\right) + e_f g m_f$$

$$A_{3,10} = I_{\omega f}\dot{\omega}_f \sin(\varepsilon) + N_f\left(l_b - \rho_f\cos(\varepsilon)\right) - g m_b z_b$$

$$A_{4,2} = -I_{\omega f}\omega_f \sin(\varepsilon) - V_x e_f m_f$$

$$A_{4,3} = I_{\omega f}\omega_f \cos(\varepsilon)$$

$$A_{4,4} = -c_\delta$$

$$A_{4,5} = I_{\omega f}\omega_f$$

$$A_{4,7} = N_f\left(-a_n k_{\alpha f} + k_{af}\cos(\varepsilon)\right)$$

$$A_{4,8} = N_f\left(a_n k_{tf}\cos(\varepsilon)\left(1 - k_{\gamma f}\right) - \rho_f\sin(\varepsilon)\right) - X_f\rho_f\cos(\varepsilon) + e_f g m_f + N_f k_{tf}\cos(\varepsilon)$$

$$A_{4,9} = k_{\gamma f}a_n N_f\sin(\varepsilon) + m_f e_f a_x\cos(\varepsilon) + A_{4,8}\sin(\varepsilon) - N_f a_n k_{\gamma f}\sin(\varepsilon)$$

$$A_{4,10} = X_f\left(a_n\sin(\varepsilon) + l_b\cos(\varepsilon) - \rho_f\cos^2(\varepsilon)\right) - m_b z_b\left(a_x\cos(\varepsilon) + g\sin(\varepsilon)\right) + I_{\omega f}\dot{\omega}_f\sin(\varepsilon) + N_f\left(k_{tf}\cos^2(\varepsilon) + l_b\sin(\varepsilon) - \rho_f\sin(\varepsilon)\cos(\varepsilon)\right) - N_f a_n k_{\gamma f}\cos(\varepsilon)$$

$$A_{5,2} = -I_{\omega f}\omega_f \cos(\varepsilon) + V_x m_b z_b$$

$$A_{5,3} = -I_{\omega f}\omega_f$$

$$A_{5,4} = -I_{\omega f}\omega_f \sin(\varepsilon)$$

$$A_{5,5} = -I_{\omega f}\omega_f \cos(\varepsilon)$$

$$A_{5,7} = N_f\left(-k_{af}\sin(\varepsilon) - k_{\alpha f} l_b\right)$$

$$A_{5,8} = N_f\left(-k_{tf}\sin(\varepsilon) + l_b\left(1 - k_{\gamma f}\right) - \rho_f \cos(\varepsilon)\right) + X_f \rho_f \sin(\varepsilon) - g m_b z_b$$

$$A_{5,9} = k_{\gamma f} l_b N_f \sin(\varepsilon) - m_b z_b a_x \cos(\varepsilon) + A_{5,8}\sin(\varepsilon)$$

$$A_{5,10} = k_{\gamma f} l_b N_f \cos(\varepsilon) + m_b z_b a_x \sin(\varepsilon) + A_{5,8}\cos(\varepsilon) - k_\beta$$

$$A_{6,1} = -\frac{k_{lr}}{N_r}$$

$$A_{6,3} = 1 - k_{\gamma r}$$

$$A_{6,6} = -\frac{V_x k_{lr}}{N_r}$$

$$A_{7,1} = -\frac{k_{lf}}{N_f}$$

$$A_{7,2} = -\frac{k_{lf} w}{N_f}$$

$$A_{7,3} = 1 - k_{\gamma f}$$

$$A_{7,4} = \left(1 - k_{\gamma f}\right)\sin(\varepsilon) + \frac{a_n k_{lf}}{N_f}$$

$$A_{7,5} = \left(1 - k_{\gamma f}\right)\cos(\varepsilon) + \left(l_b - \rho_f \cos(\varepsilon)\right)\frac{k_{lf}}{N_f}$$

$$A_{7,7} = -\frac{V_x k_{lf}}{N_f}$$

$$A_{7,9} = \frac{V_x k_{lf}\cos(\varepsilon)}{N_f}$$

$$A_{7,10} = -\frac{V_x k_{lf}\sin(\varepsilon)}{N_f}$$

$$A_{8,3} = 1$$

$$A_{9,4} = 1$$

$$A_{10,5} = 1$$

Appendix A0.1 contains all the parameters used to solve the system.

Whereas, **E** matrix is square, full rank, constant and symmetric, thus, the non-zero entries are:

$$
\begin{aligned}
E_{1,1} &= m & E_{2,2} &= mb^2 + I_{zz} \\
E_{1,2} &= mb & E_{2,3} &= mbh - I_{xz} \\
E_{1,3} &= mh & E_{2,4} &= m_f e_f b_f + I_{fzz}\cos(\varepsilon) \\
E_{1,4} &= m_f e_f & E_{2,5} &= -m_b b_b z_b - I_{bxx}\sin(\varepsilon) \\
E_{1,5} &= -m_b z_b & & \\
\\
E_{3,3} &= mh^2 + I_{xx} & E_{4,4} &= m_f e_f^2 + I_{fzz} \\
E_{3,4} &= m_f e_f h_f + I_{fzz}\sin(\varepsilon) & E_{4,5} &= -m_b e_b z_b \\
E_{3,5} &= -m_b h_b z_b + I_{bxx}\cos(\varepsilon) & & \\
\\
E_{5,5} &= m_b z_b^2 + I_{bzz} & E_{8,8} &= 1 \\
E_{6,6} &= k_{\alpha r} & E_{9,9} &= 1 \\
E_{7,7} &= k_{\alpha f} & E_{10,10} &= 1
\end{aligned}
$$

Table 3.2: Components of the Matrix E

To summarise, a comprehensive analysis of motorcycle stability has been presented, using Lot & Sadauckas (2021)' model. The detailed exploration of the model geometry provided the understanding necessary to delve into subsequent analyses. The formulation of kinematic equations and EoMs allowed the characterisation of motion and behaviour of the motorcycle. Furthermore, the model was extended to incorporate two aerodynamic considerations more, factors that may significantly influence the behaviour of the motorcycle. Thus, an integral motorcycle stability model has been constructed, offering a robust framework for future research in the field of motorcycle dynamics. This chapter serves as a guide for comprehending the motorcycle stability model and continuing its development.

Chapter 4

Cornering

In this chapter, model is modified to allow the stability study in steady cornering conditions. Along with that, new parameters and assumptions are explained. To reinforce the development of the model, the results of this chapter were compared to Cossalter et al. (1999), Schwab et al. (2005) and Cossalter (2006b).

4.1 Model modification for cornering conditions

The previous model had several linearised equations since it is supposed to be used in straight-running conditions. However, in this work, EoMs are generalised to be suitable for larger roll and steering angles. For this reason, it is necessary to introduce new diagrams to explain the complex geometry of motorcycle steering. Those detailed diagrams are crucial to understand the formulation of equations.

In addition, for steady cornering conditions, the motorcycle has an initial and constant roll angle φ_0 and an initial steering angle δ_0. To study the stability of the system, we formulate the EoMs considering the initial angle plus an oscillatory one as $\varphi_0 + \varphi$, and the same for steering angle with $\delta_0 + \delta$.

Now, with intricate geometry, new steering angles are defined, of which only two are relevant for the final model. First, the motorcycle real steering angle is called δ, which is measured in a plane orthogonal to the steering head axis. Second, the kinematic steering angle is called Δ, which is the steering angle projected to the ground.

At this point, it is important to add an explanation of the following Figures 4.1 and 4.2. First, the green-coloured plane represents the initial plane of the vehicle, in its initial

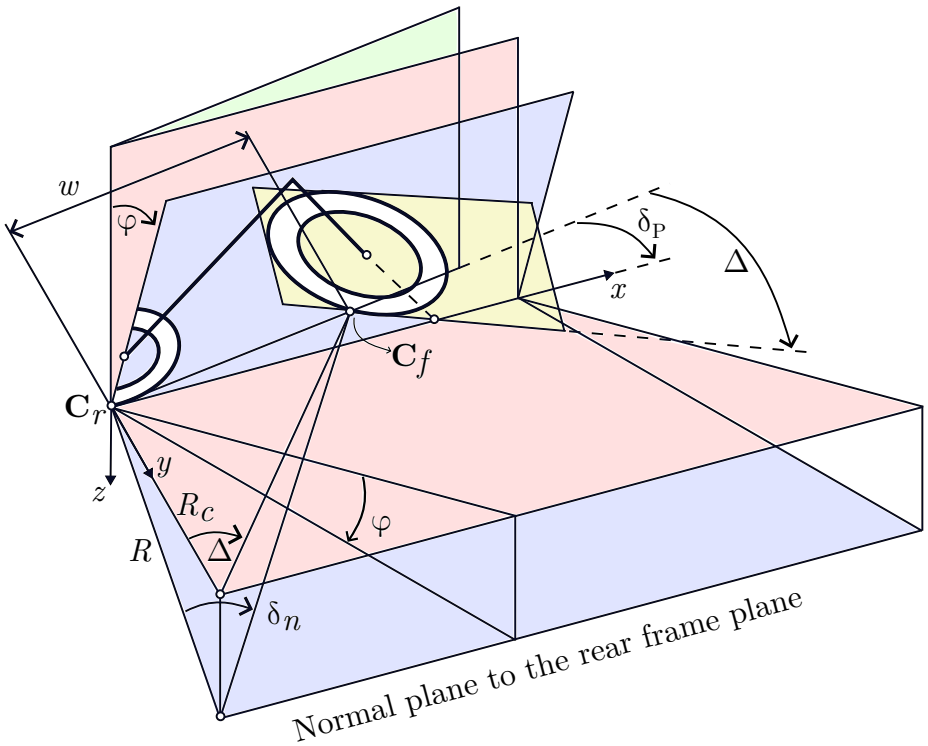

Figure 4.1: Motorcycle geometry in cornering.

position, without steering or rolling angle. Second, the red planes show the chassis plane modified only by steering angle, which represents the yaw angle ψ, as shown in Figure 4.2. Third, blue planes come from the addition of steering and rolling angle, which projects the rotation centre below the ground level as shown in Figure 4.1. Lastly, the yellow plane represents the front wheel plane, which goes out of the previously mentioned planes and intersects them.

Then, from single track vehicle geometry, it is possible to obtain the kinematic steering angle as

$$\tan(\Delta) = \frac{w}{R_c}, \tag{4.1}$$

where R_c is the path radius of the curvature.

Equally, steering angle projected to the normal plane to the rear frame plane is

$$\tan(\delta_n) = \frac{w}{R},$$

where R is the curvature radius seen in Figure 4.1.

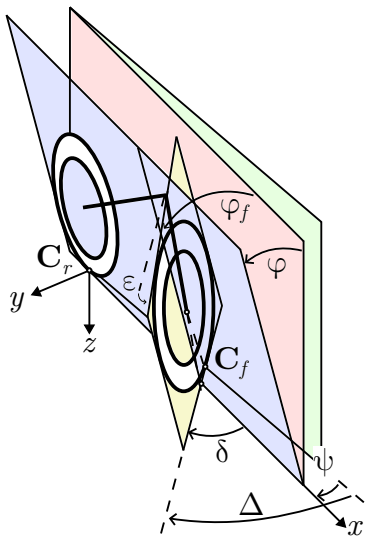

Figure 4.2: Front view of motorcycle geometry.

The relation between R and R_C is $R\cos(\varphi) = R_c$, which gives the equation

$$\tan(\delta_n) = \tan(\Delta)\cos(\varphi) = \tan(\delta)\cos(\varepsilon). \tag{4.2}$$

Then, reordering the terms and replacing Equation (4.1), it reads

$$\delta = \arctan\left(\frac{\cos(\varphi)}{\cos(\varepsilon)}\frac{w}{R_c}\right). \tag{4.3}$$

However, following equations depend on Δ, therefore it is re-written, resulting

$$\Delta = \arctan\left(\frac{\cos(\varepsilon)}{\cos(\varphi)}\tan(\delta)\right). \tag{4.4}$$

Besides, the equation for frontal roll angle is formulated from Figure 4.1 and is given by

$$\sin(\varphi_f) = \cos(\delta)\sin(\varphi) + \cos(\varphi)\sin(\delta)\sin(\varepsilon).$$

Rewritten it reads

$$\varphi_f = \arcsin(\cos(\delta)\sin(\varphi) + \cos(\varphi)\sin(\delta)\sin(\varepsilon)). \tag{4.5}$$

To formulate the equation of motorcycle rear frame roll, it is derived from roll equilibrium

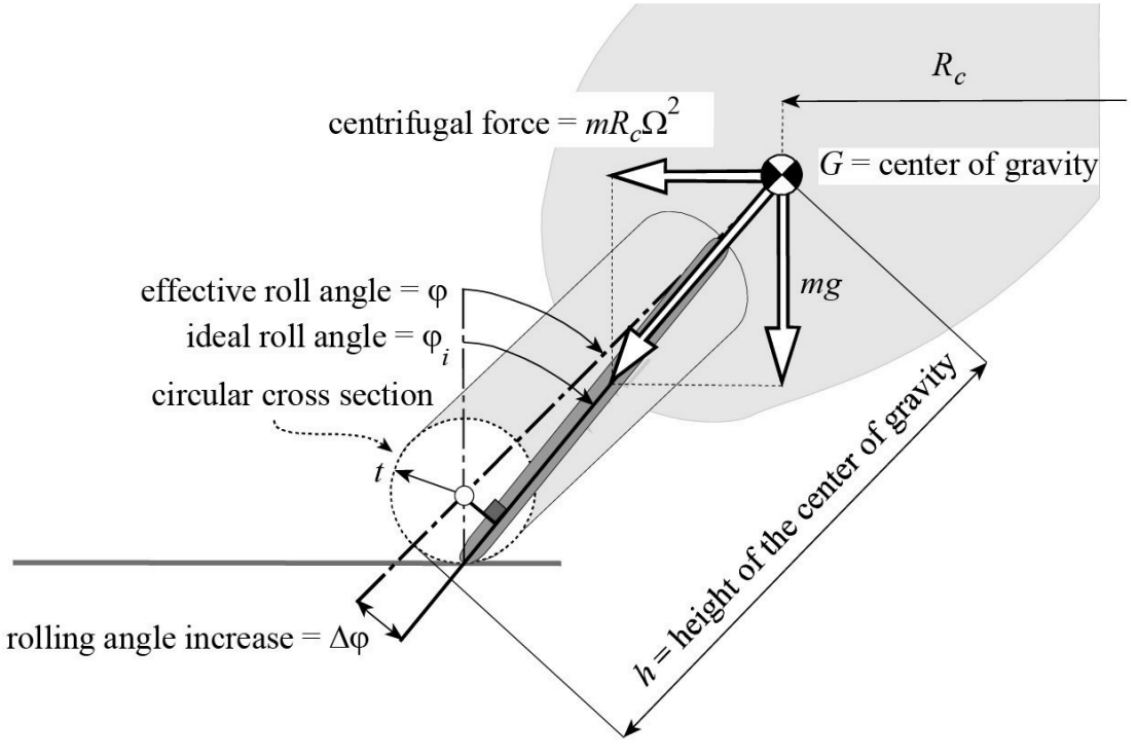

Figure 4.3: Steady turning: roll angle of the motorcycle equipped with real tires. Extracted from Cossalter (2006b).

as

$$\varphi = \arctan\left(\frac{V_x^2}{gR_c}\right),$$

where V_x is the longitudinal velocity and g is the gravitational acceleration.

However, since in this work a toroidal cross-section tyre is considered, it has effect on roll angle by

$$\Delta\varphi = \arcsin\left(\frac{\rho_r \sin(\varphi)}{h - \rho_r}\right),$$

where ρ_r is the toroidal cross-section of the rear tyre and h is the height of the motorcycle CoM.

At the end, the general roll equation reads

$$\varphi_0 = \arctan\left(\frac{V_x^2}{gR_c}\right) + \Delta\varphi, \tag{4.6}$$

which can be seen in Figure 4.3. Here, φ_0 is used to clarify the origin of the initial roll angle.

Additionally, considering tyres with toroidal cross-section implies that wheel radius changes in relation to roll angle. Therefore, it requires establishing a relation between them, first, considering the rolling radius at zero roll as $R_r - \rho_r + \rho_r cos(\varphi)$, which results in

$$\omega_r = \frac{V_x}{R_r + \rho_r(\cos(\varphi) - 1)} \tag{4.7a}$$

$$\omega_f = \frac{V_x}{(R_f + \rho_f(\cos(\varphi_f) - 1))\cos(\Delta)} \tag{4.7b}$$

where R_i are the wheel radius and ρ_i are the toroidal cross-section radius.

4.1.1 Fork bending angle β

The degree of freedom β represents the fork lateral bending, which affects the kinematic steering, the front roll angle and the front sideslip. Adding to Equation (4.2) results in

$$\begin{aligned}
\tan(\Delta)\cos(\varphi) &= \tan(\delta)\cos(\varepsilon) - \beta\sin(\varepsilon) \\
\tan(\delta)\cos(\varepsilon) &= tan(\Delta)\cos(\varphi) + \beta\sin(\varepsilon) \\
\tan(\delta) &= \frac{\cos(\varphi)}{\cos(\varepsilon)}\tan(\Delta) + \beta\tan(\varepsilon) \\
\Rightarrow \delta_0 &= \arctan\left(\frac{\cos(\varphi)}{\cos(\varepsilon)}\tan(\Delta) + \beta\tan(\varepsilon)\right).
\end{aligned} \tag{4.8}$$

Note that at the end, we use δ_0 since is the initial steering angle. That serves only as clarification about the origin of δ_0.

In line manner, Equation (4.5) results

$$\sin(\varphi_f) = \cos(\delta)\sin(\varphi) + \cos(\varphi)\sin(\delta)\sin(\varepsilon) + \beta\cos(\varepsilon)\cos(\varphi). \tag{4.9}$$

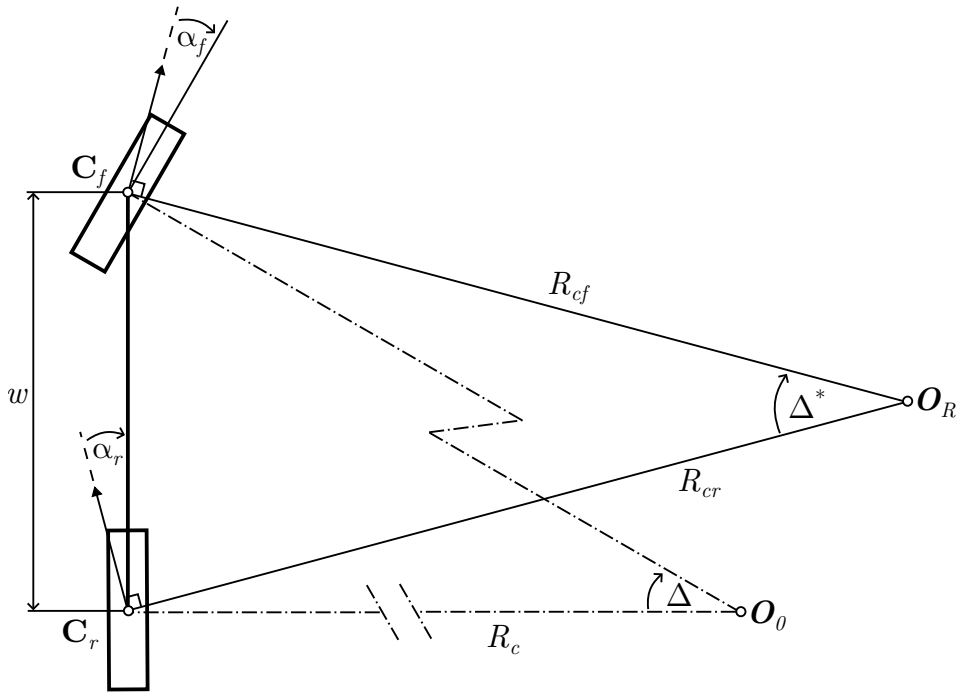

Figure 4.4: Cornering geometry with front and rear sideslip.

4.1.2 Sideslip

This model consider sideslip of the tyres, changing the geometry of cornering. Therefore, including sideslip angles to the Equation (4.1) it results

$$\Delta^* = \Delta + \alpha_r - \alpha_f, \tag{4.10}$$

where α_f and α_r are front and rear tyre sideslip respectively.

As can be seen in Figure 4.4, the turning radius of the trajectory, considering tyre sideslip is

$$R_{cr} = \frac{w}{\tan(\Delta - \alpha_f)\cos(\alpha_r) + \sin(\alpha_r)}. \tag{4.11}$$

In addition, for small sideslip angles, it can be calculated as

$$\alpha_r = -\frac{V_y}{V_x} \tag{4.12a}$$

$$\alpha_f = \Delta + \frac{a_n\dot{\delta} - w\dot{\psi} - V_y + (l_b - \rho_f\cos(\varepsilon))\dot{\beta}}{V_x}, \tag{4.12b}$$

it is important to note that in Equation (4.12b) is already included the fork bending.

Finally, due to small sideslip angles, the turning radius can be approximated by

$$R_{cr} \approx \frac{w}{\Delta} \tag{4.13}$$

4.1.3 Force description

Since larger camber angles are considered, it is necessary to capture its effect in the equations of tyre forces. By the same, it is necessary to include the lateral force due to rolling equilibrium, resulting in

$$Y_r = \left(k_{\alpha r}\alpha'_r + k_{\gamma r}\varphi_r\right) N_r \tag{4.14a}$$

$$Y_f = \left(k_{\alpha f}\alpha'_f + k_{\gamma f}\varphi_f\right) N_f. \tag{4.14b}$$

Equally, tyre yaw torques are affected by large camber angles, which now becomes

$$M_{rz} = (k_{ar}\alpha'_r + k_{tr}\varphi_r)N_r \tag{4.15a}$$

$$M_{fz} = (k_{af}\alpha'_f + k_{tf}\varphi_f)N_f. \tag{4.15b}$$

Finally, normal forces on the tyres, including aerodynamics are defined by

$$N_r = N_{r0} + \frac{h_A}{w}F_{ad} + \frac{1}{w}\left(mh + \frac{I_{\omega r}}{R_r} + \frac{I_{\omega f}}{R_f}\right)a_x + \left(1 - \frac{b_A}{w_A}\right)D\cos(\varphi_0 + \varphi) \tag{4.16a}$$

$$N_f = N_{f0} - \frac{h_A}{w}F_{ad} - \frac{1}{w}\left(mh + \frac{I_{\omega r}}{R_r} + \frac{I_{\omega f}}{R_f}\right)a_x + \frac{b_A}{w_A}D\cos(\varphi_0 + \varphi). \tag{4.16b}$$

4.2 Equilibrium of forces

Following the same formulation as Section 3.3.1, the EoMs for sum of forces are

$$ma_x = X_r + X_f\cos(\Delta) - F_{ad} - Y_f\sin(\Delta) \tag{4.17a}$$

$$m(\dot{V}_y+b\ddot{\psi}+h\cos(\varphi_0+\varphi)\ddot{\varphi}+V_x\dot{\psi})+m_f e_f\ddot{\delta}-m_b z_b\ddot{\beta} = Y_r+Y_f\cos(\Delta)+X_f\sin(\Delta)-D\sin(\varphi_0+\varphi) \tag{4.17b}$$

$$mh\sin(\varphi_0+\varphi)\ddot{\varphi} = -mg-(N_f+N_r)+D\cos(\varphi_0+\varphi), \tag{4.17c}$$

4.3 Equilibrium of moments

Again, the formulation of rotational equations works in the same way as Section 3.3.2. All of the equations are with respect to the origin of the main coordinate system, aligned with the rear wheel contact point $\mathbf{C}_r$. Due to the length of the equations, they are split into two: the inertial side and the external moments side. The inertial side is

$$(mbh-I_{xz})\ddot{\psi}+(mh^2+I_{xx})\ddot{\varphi}+(m_f e_f h_f+I_{fzz}\sin(\varepsilon))\ddot{\delta}+ (I_{bxx}\cos(\varepsilon)-m_b h_b z_b)\ddot{\beta}+mh(\dot{V}_y+V_x\dot{\psi}) = M_x \tag{4.18a}$$

$$-mha_x-mh\cos(\varphi_0+\varphi)\dot{V}_x-(I_{\omega f}\dot{\omega}_f\cos(\varphi_{0f}+\varphi_f)+I_{\omega r}\dot{\omega}_r\cos(\varphi_0+\varphi)) = M_y \tag{4.18b}$$

$$(mb^2+I_{zz})\ddot{\psi}+(mbh-I_{xz})\ddot{\varphi}+(m_f e_f b_f+I_{fzz}\cos(\varepsilon))\ddot{\delta}+ (I_{bxx}\sin(\varepsilon)-m_b b_b z_b)\ddot{\beta}+mb(\dot{V}_y+V_x\dot{\psi})+(m_b z_b\beta-mh\sin(\varphi_0+\varphi)-m_f e_f\sin(\delta_0+\delta))\dot{V}_x- I_{\omega r}(\omega_r\dot{\varphi}+\dot{\omega}_r\sin(\varphi_0+\varphi))-I_{\omega f}(\omega_f\dot{\varphi}_f+\dot{\omega}_f\sin(\varphi_{0f}+\varphi_f)) = M_z \tag{4.18c}$$

While the side of external moments of the equations is presented below

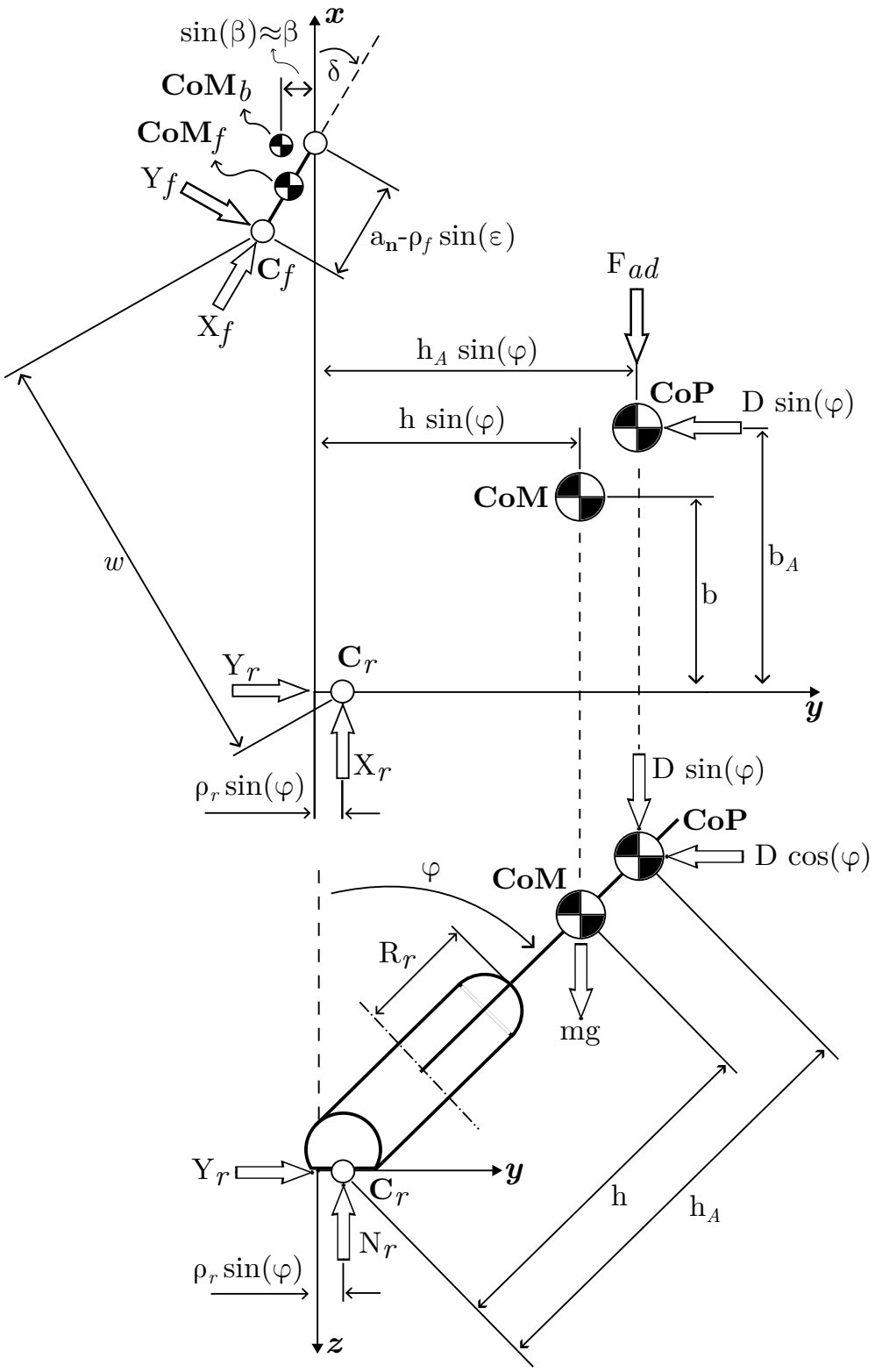

Figure 4.5: Overall geometry.

$$M_x = [(a_n - \sin(\varepsilon)\rho_f)\sin(\delta_0+\delta) + (l_b - \cos(\varepsilon)\rho_f)\beta - \rho_f \sin(\varphi_0+\varphi)]N_f \\ - \rho_r N_r \sin(\varphi_0+\varphi) + mgh\sin(\varphi_0+\varphi) - m_b g z_b \beta + m_f g e_f \sin(\delta_0+\delta) \quad (4.19a)$$

$$M_y = wN_f - bmg + (h_A F_{ad} - b_A D)\cos(\varphi_0+\varphi) \quad (4.19b)$$

$$M_z = wY_f - \rho_r X_r \sin(\varphi_0+\varphi) + (h_A F_{ad} - b_A D)\sin(\varphi_0+\varphi) + M_{rz} + M_{fz} + \\ [(a_n + \omega\cos(\varepsilon) - \rho_f \sin(\varepsilon))\sin(\delta_0+\delta) - \rho_f \sin(\varphi_0+\varphi) + (l_b - \rho_f\cos(\varepsilon) - w\sin(\varepsilon))\beta]X_f \quad (4.19c)$$

4.3.1 Steering

The steering behaviour is governed by the following equation, which is derived around the steering axis aligned with the z axis of the front system.

$$(m_f e_f^2 + I_{fzz})\ddot{\delta} + (m_f e_f h_f + I_{fzz}\sin(\varepsilon))\ddot{\varphi} - m_b e_b z_b \ddot{\beta} + (m_f e_f b_f + I_{fzz}\cos(\varepsilon))\ddot{\psi} + \\ m_f e_f(\dot{V}_y + V_x\dot{\psi} + \dot{V}_x\cos(\varepsilon)\sin(\delta_0+\delta)) + I_{\omega f}\omega_f(\dot{\psi}\sin(\varepsilon) - \dot{\varphi}\cos(\varepsilon)) - I_{\omega f}(\omega_f\dot{\beta} + \dot{\omega}_f\beta) = \\ M_\delta - c_\delta\dot{\delta} - a_n Y_f + M_{fz}\cos(\varepsilon) + [(l_b\cos(\varepsilon) + a_n\sin(\varepsilon))\beta + \rho_f\cos(\varepsilon)\sin(\varphi_{0f}+\varphi_f)]X_f + \\ + [(a_n - \rho_f\sin(\varepsilon))\sin(\varphi_{0f}+\varphi_f) + (l_b\sin(\varepsilon) + a_n\cos(\varepsilon))\beta]N_f + \\ + (a_x\cos(\varepsilon) + g\sin(\varepsilon))(m_f e_f\sin(\delta_0+\delta) - m_b z_b\beta) + g m_f e_f\sin(\varphi_0+\varphi), \quad (4.20)$$

where M_δ is the rider input torque, and c_δ is the torque generated by steering bearings friction and the action of and steering damper if it exists.

4.3.2 Fork bending

Lastly, the fork bending equation follows the same procedure as Section 3.3.2.2. Then, it reads

$$
\begin{aligned}
-(m_b b_b z_b + I_{bxx}\sin(\varepsilon))\ddot{\psi} + (I_{bxx}\cos(\varepsilon) - m_b h_b z_b)\ddot{\varphi} - m_b e_b z_b \ddot{\delta} + \\
+ (m_b z_b^2 + I_{bzz})\ddot{\beta} - m_b z_b(\dot{V}_y + V_x\dot{\psi}) + I_{\omega f}\omega_f(\dot{\varphi}_f + \dot{\psi}\cos(\varepsilon)) = \\
- l_b Y_f \cos(\varphi_{0f} + \varphi_f) - M_{fz}\sin(\varepsilon) + \\
[(l_b - \rho_f\cos(\varepsilon))N_f + \rho_f\sin(\varepsilon)X_f]\sin(\varphi_{0f} + \varphi) \\
- k_\beta\beta + m_b z_b[a_x(\beta\sin(\varepsilon) - \sin(\delta_0 + \delta)\cos(\varepsilon)) - g\sin(\varphi_{0f} + \varphi_f)], \quad (4.21)
\end{aligned}
$$

where right-hand terms are moments generated with respect to the bending axis x_b, and k_β is the bending stiffness of the fork.

To conclude, the objective of the present chapter is to extend and develop the stability model to be suitable for steady cornering conditions. In steady cornering conditions, roll and steering angles become larger, which modifies the kinematic equations. Therefore, the kinematic equations were revised and adapted, now they are suitable to consider an initial angle φ_0 and δ_0, plus oscillatory angles φ and δ, for roll and steering respectively. For a better understanding of the formulation, several diagrams for geometries and forces are presented. complementing the explanation of each equation.

Chapter 5

Conclusion

In this work, we developed a mathematical model for the lateral stability of the motorcycle. To achieve that, we studied several stability models and compared the formulation of them. Thus, the model with better documentation was replicated and extended to consider aerodynamic lift and different CoP positions. Additionally, the model was modified again to be suitable for steady cornering conditions.

In motorcycle racing, the manufacturers always look to reduce lap times, mainly by increasing the top and the cornering speed. The top speed increase requires greater accelerations, which are limited by the "wheelie" phenomenon, where the front wheel loses contact with the ground. Therefore, engineers found a solution to the phenomenon using downforce on the vehicle. However, according to the literature available, that kind of solution can produce instability on the motorcycle. Consequently, the motivation of this research was to develop a model to study motorcycle stability considering the current aerodynamic advances.

The beginning of the project was about studying the different stability models and the aerodynamics of modern MotoGP motorcycles. Alongside, it was presented a brief explanation of stability studies and particularities about motorcycle stability. Then, from the estimation of motorcycle wing characteristics, applied in aerodynamic software, the required values for the model were obtained. Thus, after a review of the two main topics of the present work, we were able to implement and develop the stability model.

The geometry of the motorcycle presented by Lot & Sadauckas (2021) was studied and revised to understand how it works. Later, a downforce component was added to the model, considering its respective CoP position, which modified several EoMs. At the end

of that chapter, the presented model was ready to be implemented and obtain preliminary results. However, that model is only valid for straight running conditions, therefore, it is necessary to modify it again.

In the last chapter, the model was upgraded to be suitable for cornering conditions, which consisted mainly of revising the kinematic equations. It also served as an opportunity to deeply understand the formulation of the inertial equations of the motorcycle. The new model was compared to other models to revise the right formulation (Cossalter, 2006b), (Schwab et al., 2005). Additionally, several detailed diagrams were made and included in the chapter to support the formulations. Thus, the model for cornering considers an initial roll and steering angle, to which is added an oscillatory angle.

To conclude, this work consisted of developing a motorcycle model to study its lateral stability. It served to understand the mechanical principles of motorcycle behaviour. The model developed is a simple one yet gives an approximation of the current tendencies in the motorcycle world. On the other hand, the formulation of the model was clearly shown, which allows a better revision and understanding of the procedures. Finally, the mathematical model developed can be implemented in software to study motorcycle stability.

Bibliography

Beeler, J. (2018). Ducati ceo tips winglets for the panigale v4 r. URL: https://www.asphaltandrubber.com/rumors/ducati-panigale-v4-r-winglet-claudio-domenicali/ accessed: 2023-07-24.

Bridges, P., & Russell, J. B. (1987). The effect of topboxes on motorcycle stability. *Vehicle System Dynamics*, *16*, 345–354.

Cathcart, A. (2013). Der spektakuläre grand-prix-achtzylinder. URL: https://www.motorradonline.de/klassiker/moto-guzzi-500-v8-der-spektakulaere-grand-prix-achtzylinder/ accessed: 2023-07-24.

Cheli, F., Bocciolone, M., Pezzola, M., & Leo, E. (2006). Esda2006-95311 numerical and experimental approaches to investigate the stability of a motorcycle vehicle.

Cooper (1983). The effect of handlebar fairings on motorcycle aerodynamics. *SAE Technical Paper*, .

Cossalter, V. (2006b). *Motorcycle Dynamics Second Edition*.

Cossalter, V., Doria, A., & Lot, R. (1999). Steady turning of two-wheeled vehicles. *Vehicle System Dynamics*, *31*, 157–181. doi:10.1076/vesd.31.3.157.2013.

Cossalter, V., & Lot, R. (2002). A motorcycle multi-body model for real time simulations based on the natural coordinates approach. *Vehicle System Dynamics*, *37*, 423–447.

Cossalter, V., Lot, R., & Maggio, F. (2002b). The influence of tire properties on the stability of a motorcycle in straight running and curves reprinted from: Proceedings of the 2002 sae automotive dynamics and stability conference and exhibition (p-377) sae automotive dynamics and stability conference and exhibition detroit, michigan.

Cossalter, V., Lot, R., & Maggio, F. (2004). The modal analysis of a motorcycle in straight running and on a curve. *Meccanica*, *39*, 1–16.

Cossalter, V., Lot, R., & Massaro, M. (2007). The influence of frame compliance and rider mobility on the scooter stability. *Vehicle System Dynamics*, *45*, 313–326.

Cossalter, V., Lot, R., & Massaro, M. (2011). An advanced multibody code for handling and stability analysis of motorcycles. *Meccanica*, *46*, 943–958.

Dijck, T. V. (2015). Computational evaluation of aerodynamic forces on a racing motorcycle during high speed cornering. SAE International volume 2015-March.

Fialho, F. (2023). Gallery: Picture of the brand new aprilia rs-gp 2023. URL: https://www.motorcyclesports.net/articles/gallery-picture-of-the-brand-new-aprilia-rs-gp-2023 accessed: 2023-07-24.

Foale, T. (2002). *Motorcycle Handling and Chassis Design the art and science*. URL: www.tonyfoale.com.

Gonzalez, B. E. (2023). Implementación de un modelo matemático para estudiar la estabilidad de las motocicletas.

Iwanbanaran (2023). Bertabur sponsor indonesia, inilah new gresini 2023 motogp team !! URL: https://www.iwanbanaran.com/2023/01/22/mega-gallery-bertabur-sponsor-indonesia-inilah-new-gresini-2023-motogp-team/ accessed: 2023-07-24.

Kamalakkannan, K., Shreyas, V. S., & Raj, J. G. (2020). Drag induced aerodynamic braking for racing motorcycles. (pp. 6870–6873). Elsevier Ltd volume 45.

Kane, T. R. (1979). The effect of frame flexibility on high speed weave of motorcycles, .

Keogh, J., Doig, G., Diasinos, S., & Barber, T. (2015). The influence of cornering on the vortical wake structures of an inverted wing. *Proceedings of the Institution of Mechanical Engineers, Part D: Journal of Automobile Engineering*, *229*, 1817–1829.

Koenen, C., & Pacejka, H. B. (1982). The influence of frame elasticity, simple rider body dynamics and tyke moments on free vibrations of motorcycles in curves, .

Lot, R., & Lio, M. D. (2004). A symbolic approach for automatic generation of the equations of motion of multibody systems.

Lot, R., & Sadauckas, J. (2021). *Motorcycle Design: Vehicle Dynamics, Concepts and Applications*. (1st ed.).

McLaren, P. (2023). Portimao motogp test: Yamaha's rear wing: 'my mechanics said, 'sorry, but i hope it's not working!". URL: https://www.crash.net/motogp/news/1021977/1/yamaha-s-rear-wing-my-mechanics-said-sorry-i-hope-its-not-working/ accessed: 2023-07-24.

Meijaard, J. P., & Popov, A. A. (2006). Influences of aerodynamic drag, the suspension system and rider's body position on instabilities in a modern motorcycle. *Vehicle System Dynamics*, *44*, 690–697.

Pednekar, K. P. (2021). Structural analysis of active winglet for motorcycle. *International Journal for Research in Applied Science and Engineering Technology*, *9*, 1927–1938.

Ramanujam, M. (2023). 2023 motogp: Ktm red bull factory racing unveiled. URL: https://paultan.org/2023/01/26/2023-motogp-ktm-red-bull-factory-racing-unveiled/ accessed: 2023-07-24.

Repsol, B. (2023). The honda nsr500 engine evolution. URL: https://www.boxrepsol.com/en/technology/the-honda-nsr500-engine-evolution/ accessed: 2023-07-24.

Schwab, A. L., Papadopoulos, J., Schwab, A. L., Meijaard, J. P., & Papadopoulos, J. M.

(2005). A multibody dynamics benchmark on the equations of motion of an uncontrolled bicycle. URL: https://www.researchgate.net/publication/228783829.

Scott, J. (2004). Aerospaceweb.org - drag coefficient & lifting line theory. URL: https://aerospaceweb.org/question/aerodynamics/q0184.shtml accessed: 2023-07-24.

Scott, M. (2008). Motogp: Ducati - no new bike in the pipeline. URL: https://www.visordown.com/news/racing/general/motogp-ducati-no-new-bike-pipeline accessed: 2023-07-24.

Scott, M. (2019). U-turn to victory: the story of the honda nsr500. URL: https://www.goodwood.com/grr/race/historic/2019/6/u-turn-to-victory-the-story-of-the-honda-nsr500/ accessed: 2023-07-24.

Sedlak, V., Talamelli, A., & Wallin, S. (2012). Motorcycle cornering improvement: An aerodynamical approach based on flow interference a master thesis in fluid mechanics.

Shames, I. H. (1999). *Mecánica para ingenieros.*. URL: https://search.ebscohost.com/login.aspx?direct=true&AuthType=sso&db=cat09074a&AN=cbu.oai.edge.bibliotecasudec.folio.ebsco.com.fs00001060.7009ac2c.81f4.4b6b.9f35.660fca5c5284&lang=es&site=eds-live&scope=site&custid=s7489523.

Sharma, A., & Limebeer, D. J. (2012). Dynamic stability of an aerodynamically efficient motorcycle. (pp. 1319–1340). volume 50.

Sharp, R. S. (1971). The stability and control of motorcycles, .

Sharp, R. S. (1974). Research note: The influence of frame flexibility on the lateral stability of motorcycles, .

Shea, T. (2018). 1966 honda rc 166. URL: https://www.hemmings.com/stories/article/1966-honda-rc166 accessed: 2023-07-24.

Appendix A

Motorcycle parameters

Parameter	Value	Units	Description
w	1.448	m	Wheelbase
ε	26.8	°	Caster angle
a_n	0.105	m	Mechanical trail
m_0	195	kg	Vehicle mass
b_0, h_0	0.722, 0.482	m	Centre of mass (CoM) position
I_{0xx}, I_{0xz}, I_{0zz}	13.5, 3, 55	kgm^2	Moments of inertia
m	270	kg	Overall mass (with 75 [kg] rider)
b, h	0.688, 0.64	m	Overall CoM position
I_{xx}, I_{xz}, I_{zz}	35.5, -1.7, 59.3	kgm^2	Overall moments of inertia
m_f	34	kg	Front assembly mass
e_f, h_f	0.025, 0.6	m	Front CoM coordinates
x_f, x_b	0.5, 0.155	m	Front and Bending CoM longitudinal position
I_{fzz}	0.83	kgm^2	Front moment of inertia
$I_{\omega f}$, $I_{\omega r}$	0.6, 0.8	kgm^2	Front and rear wheel spin inertia
c_δ	1	Nms/rad	Steering damper
R_f, R_r	0.294, 0.299	m	Front and rear rolling radius
ρ_f, ρ_f	0.064, 0.078	m	Tyre cross-section radius
$k_{\alpha f}$, $k_{\alpha r}$	16, 14.5	1/rad	Normalised cornering stiffness
$k_{\varphi f}$, $k_{\varphi r}$	0.85, 0.95	1/rad	Normalised camber stiffness
k_{af}, k_{ar}	-0.2, -0.2	m/rad	Normalised self-aligning stiffness
k_{tf}, k_{tr}	0.015, 0.018	m/rad	Normalised twist stiffness
k_{lf}, k_{lr}	160000, 140000	N/m	Transverse structural stiffness
l_β	0.67	m	Fork bending axis position
k_β	38	kNm/rad	Bending stiffness
m_b	18	kg	Bending mass
e_b, h_b	0, 0.35	m	CoM coordinates
I_{bxx}, I_{bzz}	0.8, 0.8	kgm^2	Bending mass moments of inertia
$c_D A$	0.467	m^2	Aerodynamic drag factor
h_A	0.35	m	Aerodynamic centre height

Table A0.1: Vehicle parameters: Sport touring motorcycle